2019/10/15
For Administrative Use Only

PROJECT FINAL REPORT

Project overview

1. CCITF project ID: CTD 2018-001
2. Project title: Refining the design approach for GeoExchange system
3. Name and contact information of the Principal Investigator: Dr. Wei Victor Liu, Assistant Professor, P.Eng. Email: victor.liu@ualberta.ca Phone: 780-248-5649
4. Name of CCITF Project Advisor: Maureen Kolla
4. Project start date: (2018/09/15)
5. Project completion date: (2019/09/15)
6. Final report submission date: (2019/10/15)

Executive Summary

In Alberta, new buildings have also been increasingly utilizing the GeoExchange system, which uses the shallow ground—mostly less than 150 meter—as an energy reservoir for space cooling and heating. In the system, the borehole heat exchanger (BHE) is the most crucial one because the efficiency of the GeoExchange system relies primarily on the thermal interactions between BHE and its surrounding ground. Currently, the design approach of BHE is to use analytical solutions of heat conduction governing equations under the Laplace transform (*g*-functions). However, these models do not consider the impact of both groundwater flow and buried depth on the thermal performance of BHE. This impact is beneficial because the advection of groundwater helps the dissipation of heat in the ground and therefore provides a synergistic effect on the performance of BHE under both cooling and heating modes. Consequently, this design length of BHE can be shortened, and the drilling and installation costs can be reduced substantially.

1. Project Description

1.1 Introduction and background

In Alberta, new buildings have also been increasingly utilizing the GeoExchange system, which uses the shallow ground—mostly less than 150 meter—as an energy reservoir for space cooling and heating. The GeoExchange system provides higher energy efficiency and lower electricity consumption, resulting in a substantial reduction of GHG (greenhouse gas) emissions. According to the US Department of Energy, GeoExchange system is endorsed to be "among the most efficient and comfortable heating and cooling technologies."

However, the high capital costs—associated with drilling and installation—lead to a relatively long payback period (i.e., between <10 and 20 years), which impedes the application of GeoExchange system. To reduce the capital costs, one straightforward solution is to reduce the borehole length while maintaining the required heating/cooling capacity. This is because the drilling and installation costs depend on the borehole length—a shorter borehole length means lower capital costs. This reduction of borehole length can be achieved during the design of GeoExchange system, which can be refined by including the synergistic effect of groundwater on the borehole heat exchanger (BHE).

In the GeoExchange system, BHE is the most crucial one because the efficiency of the GeoExchange system relies primarily on the thermal interactions between BHE and its surrounding ground. Currently, the design approach of BHE is to use analytical solutions of heat conduction governing equations under the Laplace transform. However, these models do not consider the impact of groundwater flow on the thermal performance of BHE. This impact is beneficial because the advection of groundwater helps the dissipation of heat in the ground and therefore provides a synergistic effect on the performance of BHE under both cooling and heating modes.

1.2 Technology description

The GeoExchange system typically consists of three components—a heat pump, a borehole heat exchanger (BHE), and a distribution circuit [1]. Among these components, BHE is the most crucial one because the efficiency of the GeoExchange system relies primarily on the thermal interactions between BHE and its surrounding ground [2]. That is, a proper design of the BHE is the key to the success of projects involving the GeoExchange system. In engineering practice, consulting firms usually use commercial software packages to design the BHE. During the design, a thermal modeling is carried out based on provided inputs (i.e., thermal properties of ground and weather conditions). These software packages often use the analytical solutions of heat conduction governing equations under the Laplace transform—two common solutions are the cylindrical source model [3] and the line source model [4]. However, these models do not consider the impact of groundwater flow on the thermal performance of BHE. This impact is beneficial because the advection of groundwater helps the dissipation of heat in the ground and therefore provides a synergistic effect on the performance of BHE under both cooling and heating modes [5]. Consequently, this design length of BHE can be shortened, and the drilling and installation costs can be reduced substantially. To this end, there is a need to refine the current design approach by incorporating the influence of groundwater. One possible solution is the use of numerical methods (i.e., finite element method—FEM) to run a co-simulation of groundwater flow with the heat transfer between BHE and its surrounding ground. In this research, we propose research to conduct FEM and analytical modeling of the BHE. This

modeling can provide very useful information (i.e., the influence of groundwater) to the designer of the GeoExchange system. As a result, a more explicit understanding will be achieved on the complex thermal behavior of BHE, and the current analytical design approach will be refined for the GeoExchange system, leading to more economically feasible design.

1.3 Project goals

The overall object of this study is to consider both groundwater and buried depth in analytical solutions to refine the current design approach for GeoExchange system.

1.4 Work scope overview

The overall work scope is to conduct a FEM (finite element method) numerical modeling on the thermal behaviors of borehole heat exchanger (BHE) in the GeoExchange system. Also, the influence of groundwater flow will be quantitatively examined through comparative studies between analytical and numerical models, leading to a newly refined design approach.

2. Outcomes and Learnings

2.1 Literature review

In general, GeoExchange or GSHP system has two common layouts—one that is horizontal and one that is vertical [6]. In comparison with the horizontal layout, the vertical layout requires a relatively smaller ground area, has a more stable heat source, and provides more efficient performance [6, 7]. In a vertical GSHP system, the heat pump is normally combined with a set of borehole heat exchangers (BHEs). These BHEs are used for heat extraction from (or injection into) the subsurface [2]. The most common form of BHE is a vertical closed loop system that has single U-tubes made of high-density polyethylene pipes. These pipes are installed into multiple vertical boreholes down to a depth ranging from 50 m to 150 m [8]. Boreholes are typically 0.1 m to 0.15 m in diameter [9]. The performance of BHE is crucial to the success of the GSHP system because it determines the amount of thermal energy extraction from the ground [10]. For a successful GSHP system, the performance of the BHE is required for satisfying thermal energy demand of a project during the life cycle of the system [10].

To evaluate the long-term performance of BHE, an approach using the *g*-function, also known as thermal response factor, is widely accepted. The *g*-function is determined by the following relationship [11]:

$$\Delta T = T_b - T_0 = \frac{q_l}{2\pi k} \times g\left(x_1, x_2, \cdots\right) \tag{1}$$

where, T_b [K] is the borehole wall temperature; T_0 [K] is the undisturbed ground temperature; q_l [Wm^{-1}] is the rate of heat production or withdrawal per unit length; k [$Wm^{-1}K^{-1}$] is the ground thermal conductivity; $g\left(x_1, x_2, \cdots\right)$ is the *g*-function; and x_1, x_2 are several non-dimensional parameters, such as non-dimensional time and non-dimensional borehole radius. The *g*-function is the non-dimensional temperature variation ($\overline{\Theta}$), averaged over the borehole wall surface, in response to a time-constant heat transfer rate in a single BHE [1, 12]:

$$g\left(x_1, x_2, \cdots\right) = \overline{\Theta} = \frac{2\pi k \Delta T}{q_l} \tag{2}$$

The *g*-function approach is widely used for two reasons. First, since the *g*-function is non-dimensional, it is convenient for a wide range of ground thermal properties and borehole geometries with equal non-dimensional parameters. For example, the same *g*-function can be valid for boreholes with various lengths (*H*) and radiuses (r_b), as long as these boreholes have the same non-dimensional borehole radius (r_b/H). Second, *g*-functions can be computed to consider thermal interactions between multiple boreholes with the help of the spatial superposition principle [11, 13]. The temporal superposition principle can also be employed to consider the time-dependent heat flux due to variations in cooling and heating loads of projects [12]. In this regard, the *g*-function methodology has been implemented commonly in GSHP design tools, such as GLHEPRO [14] and Earth Energy Designer (EED) [15]. The available *g*-functions, different are obtained through, numerical models [16-19], analytical models [4, 20-24], or a combination of the two [11, 25]. In engineering practice, analytical models are generally favored over numerical models for sizing, optimizing, and simulating the BHE system [26-29]. Advantages to the analytical approach include (1) the flexibility for any BHE geometries and configurations, (2) the superior computational time within an acceptable accuracy, and (3) the simplicity for the designers [23, 30]. This paper emphasizes *g*-functions obtained from analytical models. For clarification, the *g*-function used in this paper is for a single borehole. Results regarding *g*-functions for multiple boreholes will be detailed in a future publication.

Most analytical models for computing *g*-functions [21, 22, 31, 32] evolved from line source theory [33]. The term "line source" refers to a continuous series of point heat sources along a straight line with a constant heat flux per unit length (q_l) [33]. In practice, the borehole can be assumed to be a line source because the radius of the borehole (e.g., r_b = 0.045 m) is tiny when compared with its length (e.g., H = 70 m) [20]. Considering the borehole as a constant line source with a finite length, Eskilson [11] proposed the finite line source model (FLS). In the FLS model, the ground is regarded as a semi-infinite medium by assuming that the interface between ambient air and ground surface is maintained at a constant temperature, i.e. the undisturbed ground temperature T_0. Setting a virtual heat sink above the ground surface, the constant temperature boundary condition at the surface is compiled by the symmetrical distribution of line heat source and sink. Zeng et al. [20] later constructed an analytical solution of the FLS model in the form of a single integral that gives the temperature variation (ΔT) at any later time at a point of the surrounding ground. This is accomplished by integrating the contributions of all the continuous point sources on the line heat source and sink. To estimate the average borehole wall temperature variation, the solution proposed by Zeng et al. [20] requires one additional integration at the borehole radius (r_b) over the borehole length (*H*). Accordingly, this double integration results in a remarkable increase of computational efforts. Lamarche and Beauchamp [21] later presented another expression for the analytical *g*-function that simplified the FLS solution from a double integral into a single integral. This simplification considerably reduced the computational time by a factor of 1000 times [21].

The analytical model has subsequently been further explored to reflect myriad practical conditions in BHE design. These aspects include, but are not limited to, buried depth [22, 32], groundwater flow [23, 24], ground surface temperature [4, 34], multiple ground layers [30, 35], and borehole wall boundary condition [36, 37]. Among these aspects, buried depth and groundwater flow are of particular importance in BHE design. These aspects are briefly reviewed below.

Buried depth

Buried depth (D) is the distance from the ground surface to the starting point of the active borehole [38]. This distance is taken as zero in the FLS solutions by Lamarche and Beauchamp [21]. However, buried depth varies in different geological environments and climate regions. In cold regions (e.g., Canada, Northern Europe), ground temperature can drop below the freezing point of groundwater [39]. Therefore, BHEs are normally buried deeper in cold regions than in warm regions to avoid the associated risk of freeze-thaw cycles in the seasonally frozen ground [40]. As the buried depth increases, the thermal resistance of the ground layer above the boreholes increases, which diminishes the heat flow between the ground surface and the BHE [32]. To address these effects, Claesson and Javed [22] proposed another single integral solution of the FLS model which takes buried depth into account. The effects of buried depth from zero to infinity have been examined based on the solution of the FLS model [32] and that of the finite cylinder source model [41]. Their results show that the temperature variation caused by buried depth is relatively small for a single deep borehole, but it becomes conspicuous for a field of multiple shallow boreholes [32, 41]. In summary, buried depth is a significant aspect in BHE design, and it has been considered in some available FLS solutions.

Groundwater flow

In addition to buried depth, another significant aspect in BHE design is groundwater flow. According to local geological and hydraulic conditions, groundwater flow rates vary from metres per year to metres per day [5]. Groundwater flow is found in many geological environments, and it can considerably change the temperature regime around a borehole [26, 42]. Where groundwater exists, the heat exchange between the borehole and the ground is inherently coupled with gross heat advection by the movement of groundwater, providing a synergistic effect on the thermal performance of BHE. This synergistic effect can shorten the design length of BHE without sacrificing performance [43-45]. The effect of groundwater flow has been addressed by Sutton et al. [46] and Diao et al. [5], who presented an analytical solution of the moving infinite line source (MILS) model in a saturated porous medium with groundwater advection. With the moving heat source theory, the MILS model was developed using the effective thermal transfer velocity (U) in place of the moving speed of the heat source. Later, using the same theory as the MILS model, Molina-Giraldo et al. [23] developed a general solution of a moving finite line source model (MFLS), which takes the finite length of the borehole into consideration. Similar to the FLS solution by Zeng et al. [20], the MFLS solution by Molina-Giraldo et al. needs to be integrated over the borehole length and the borehole circumference for the average borehole wall temperature. Therefore, inspired by Lamarche and Beauchamp [21], Tye-Gingras and Gosselin [24] reformulated the triple integral formulation to be an alternative single integral expression that describes the integral mean borehole wall temperature. To summarize, the groundwater flow is another significant aspect in BHE design. This aspect is addressed in the available MFLS model.

In general, buried depth and groundwater flow both influence the long-term performance of BHE, and their effects have been considered in the available FLS and MFLS solutions, respectively. No work, however, has been done that incorporates both the effects of buried depth and groundwater flow at the same time in a single analytical model. The objective of the present study is to provide a new single integral solution that extends the validity of the MFLS model considering buried depth (MFLSD). In this model, both groundwater and buried depth can be considered in the design of GeoExchange system.

2.2 Methodology

A new analytical solution of the MFLS model (MFLSD) is presented. Inspired by the FLS solution by Claesson and Javed [22], the MFLSD solution is derived in a single integral form with respect to buried depth. To numerically verify the MFLSD solution, a three-dimensional (3D) finite element (FE) model was constructed using the software COMSOL Multiphysics. The 3D-FE solution solves the same heat transfer problem as the MFLSD solution using the input parameters from GeoExchange project in Edmonton, Alberta, Canada. The discrepancy between the two solutions is evaluated using the mean absolute error (MAE) and the root mean square deviation (RMSD). A one percent (1%) difference is employed as a criterion to decide whether the effects of buried depth are negligible. When the discrepancy between the MFLSD solution and the MFLS solution is greater than 1%, the *g*-function must be computed using the MFLSD solution to include the effects of buried depth. A general flowchart is shown below:

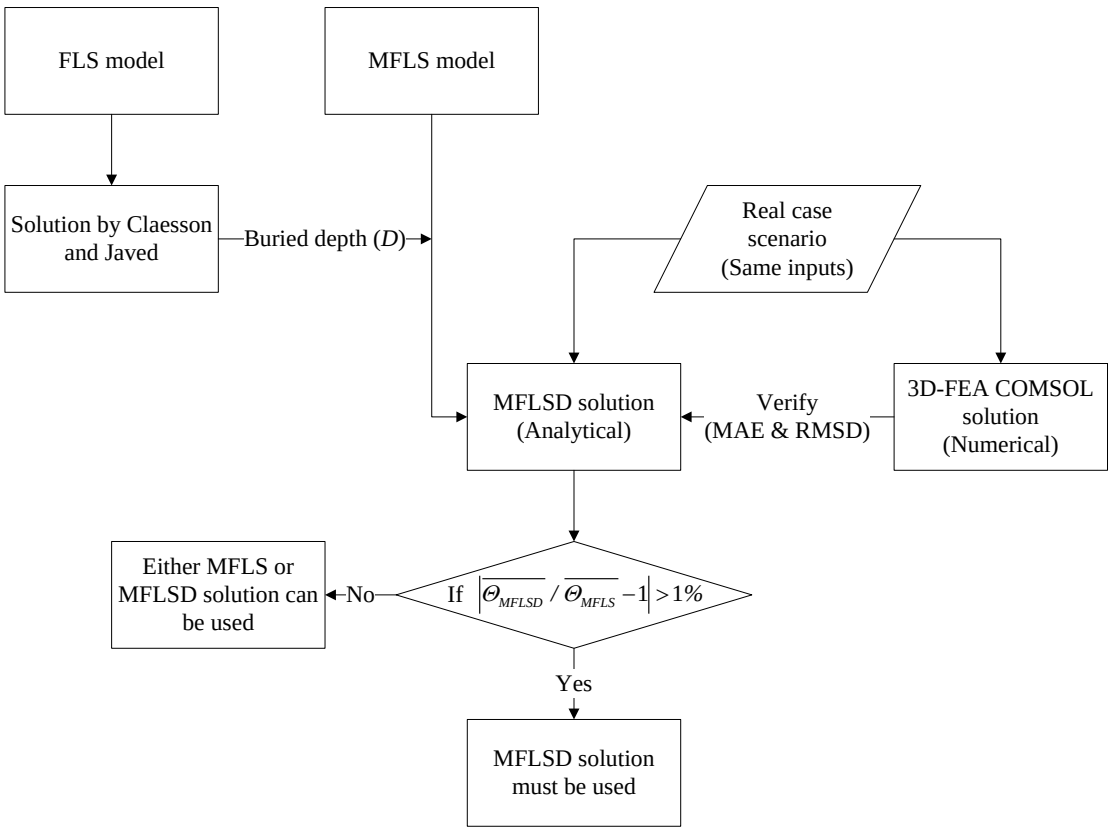

2.3 Modelling details

Model domain and mesh selection

A preliminary analysis has been done to ensure the simulation results are independent from the model domain and the mesh geometry. Guided by the work of Molina-Giraldo et al. [23], the domain dimension was enlarged starting from a horizontal domain size of (x = 200 m) × (y = 50 m) with a thickness of (z = 130 m), until the maximum temperature changes at the external boundaries are less than 0.005 °C at the end of the simulations. In principle, the temperature at the far boundary is supposed to be kept in an undisturbed condition; the selected 0.005 °C tolerance assures a reasonable domain size and preserves the calculation accuracy [13].

The maximum temperature changes at the external boundaries are tabulated in Table 1 for each domain size. The domain extensions were first determined in a pure heat conduction scenario (Pe = 0) with a buried depth of 8 m. After that, a uniform groundwater flow was assigned throughout the entire domain aligned with the x-axis. Due to the influence of groundwater flow, the model domain was further extended in the positive x-direction. Finally, the 3D-FE model was constructed with a domain size of (x = 800 m) × (y = 200 m) × (z = 320 m). Worth noting is that the reliability of the domain size was also verified by comparing the average temperature at the borehole wall, which has relative differences of less than 1% in the last extension.

Table 1 The maximum temperature changes at the boundaries of the COMSOL model.

Negative x-direction and y-direction	50 m	100 m	150 m	200 m
Maximum temperature (°C)	3.0468	0.3736	0.0436	0.0036
z-direction	130 m	180 m	230 m	280 m
Maximum temperature (°C)	1.1026	0.1487	0.0149	0.0010
Positive x-direction	200 m	400 m	600 m	
Maximum temperature (°C)	0.5243	0.0096	0.0002	

Regarding the mesh, extremely fine elements were chosen near the borehole, and coarser elements were chosen at further locations to reduce mesh numbers. Tye-Gingras and Gosselin [24] suggested that a mesh-independent solution can be obtained when doubling the number of meshes yields a relevant difference of less than 1% for the results at every time step. Therefore, a comparison of average borehole wall temperatures was carried out with an increasing number of elements on the borehole wall boundary. In our case, when the number of elements of the domain doubled from about one million to two million, the maximum difference of the average borehole wall temperature is about 0.04% (between 35.52 °C and 35.65 °C) in the considered time domain. This difference is acceptable since it is far less than 1%. Finally, the mesh geometry with about two million (2,000,000) elements was selected, which assures a reasonable number of elements and preserves calculation accuracy.

2.4 Results, analysis, and discussion of model simulations

2.4.1 Verification of the MFLSD model

A comparison between the MFLSD solution and numerical solution was conducted. As shown in Fig. 1, $\overline{\Delta T}$ was plotted against the Fourier number (Fo) for three buried depths (D = 0 m, D = 2

m, and D = 8 m) and two Peclet numbers (Pe = 0 and Pe = 7.5). It was shown that the MFLSD solution presents a good agreement with the numerical solution generated with COMSOL Multiphysics over 100 years of continuous operation. Table 2 shows that, for the given parameter of this section, the MAE and RMSD yield values of about 0.01 and 0.01 respectively, which are lower than the thresholds of the acceptable MAE (0.02) and RMSD (0.02). Therefore, the MFLSD solution was considered to be numerically verified.

In addition, a comparison with the MFLS solution of Tye-Gingras and Gosselin [24] and the FLS solution of Claesson and Javed [22] was also carried out. The MFLSD solution is identical with the MFLS solution for D = 0 m (Fig. 4a and 4d), and it is also identical with the FLS solution for Pe = 0 (Fig. 1a, 1b, and 1c). For Pe = 7.5, the MFLSD and FLS solutions (Fig. 1d, 1e, and 1f) start to differ by about 1% after two-year operation, and the dispersion became larger as the simulation time increased. Compared with the FLS results, the temperature variations from the MFLSD solution were smaller, i.e. about 8.70%, 9.01%, and 9.82% for D = 0 m, 2 m, and 8 m at 100 years, respectively. These reductions can be explained by the effects of groundwater flow, through which accumulated heat at the borehole is broadly distributed [47]. For D = 8 m, results from the MFLSD solution were greater by about 3.15% and 1.88% for Pe = 0 and Pe = 7.5 at 100 years (Fig. 1c and 1f), respectively than the MFLS results. These differences indicate that neglecting buried depth can underestimate the temperature variation. The underestimation is caused by the thermal resistance of the ground layer between the ground surface and BHE. The thermal resistance diminishes the changes in temperature [32]. In general, both buried depth and groundwater flow change the temperature variations in the long term. When incorporating the effects of buried depth and groundwater flow at the same time (Fig. 1e and 1f), the MFLSD model gives a better prediction of temperature variation. As shown in Table 2, MSRD always yields to a smaller value for the MFLSD model.

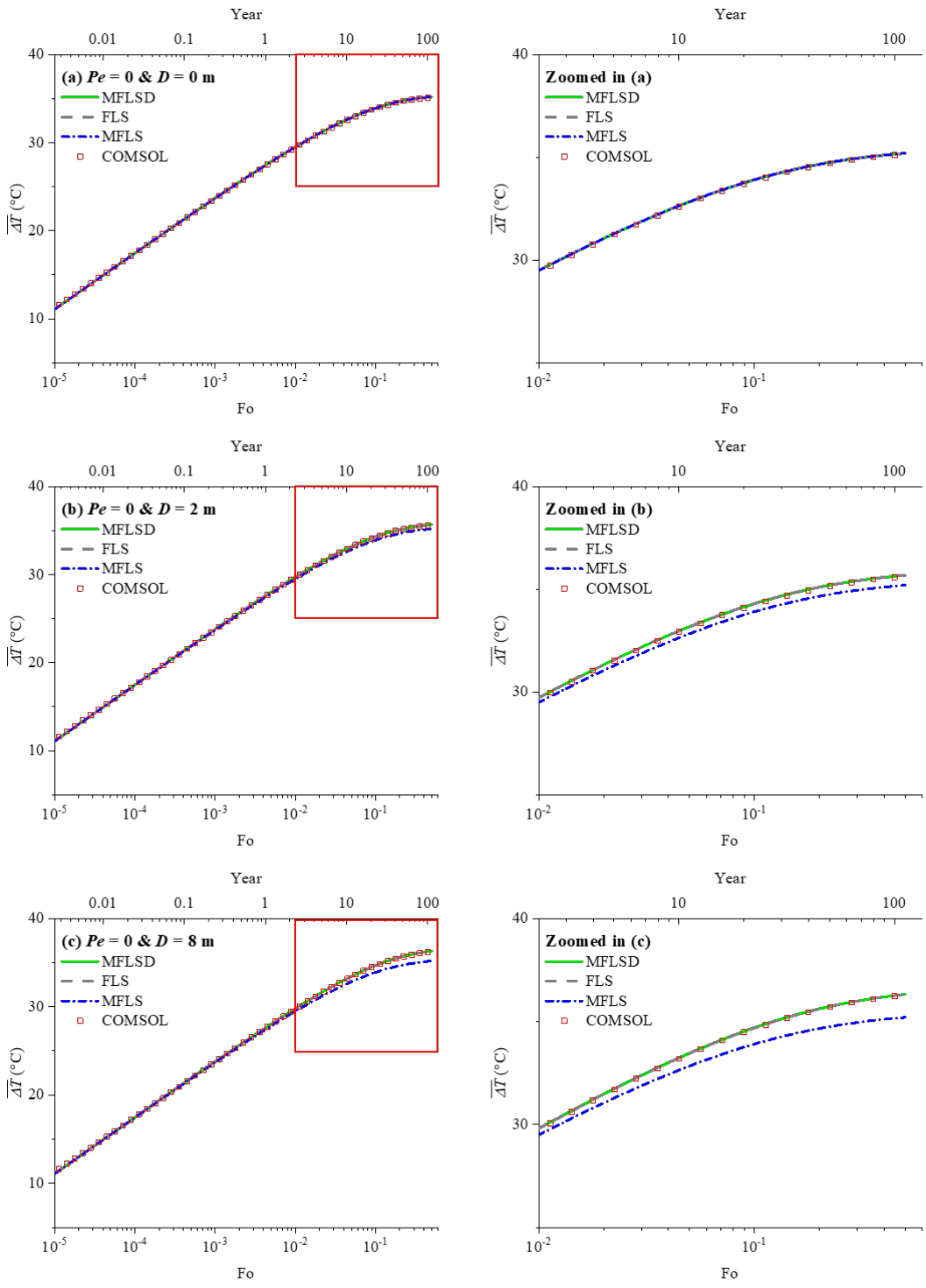
Year
0.01
0.1
1
10
100
(a) Pe = 0 & D = 0 m
MFLSD
FLS
MFLS
COMSOL
ΔT (°C)
Fo
Zoomed in (a)
(b) Pe = 0 & D = 2 m
Zoomed in (b)
(c) Pe = 0 & D = 8 m
Zoomed in (c)

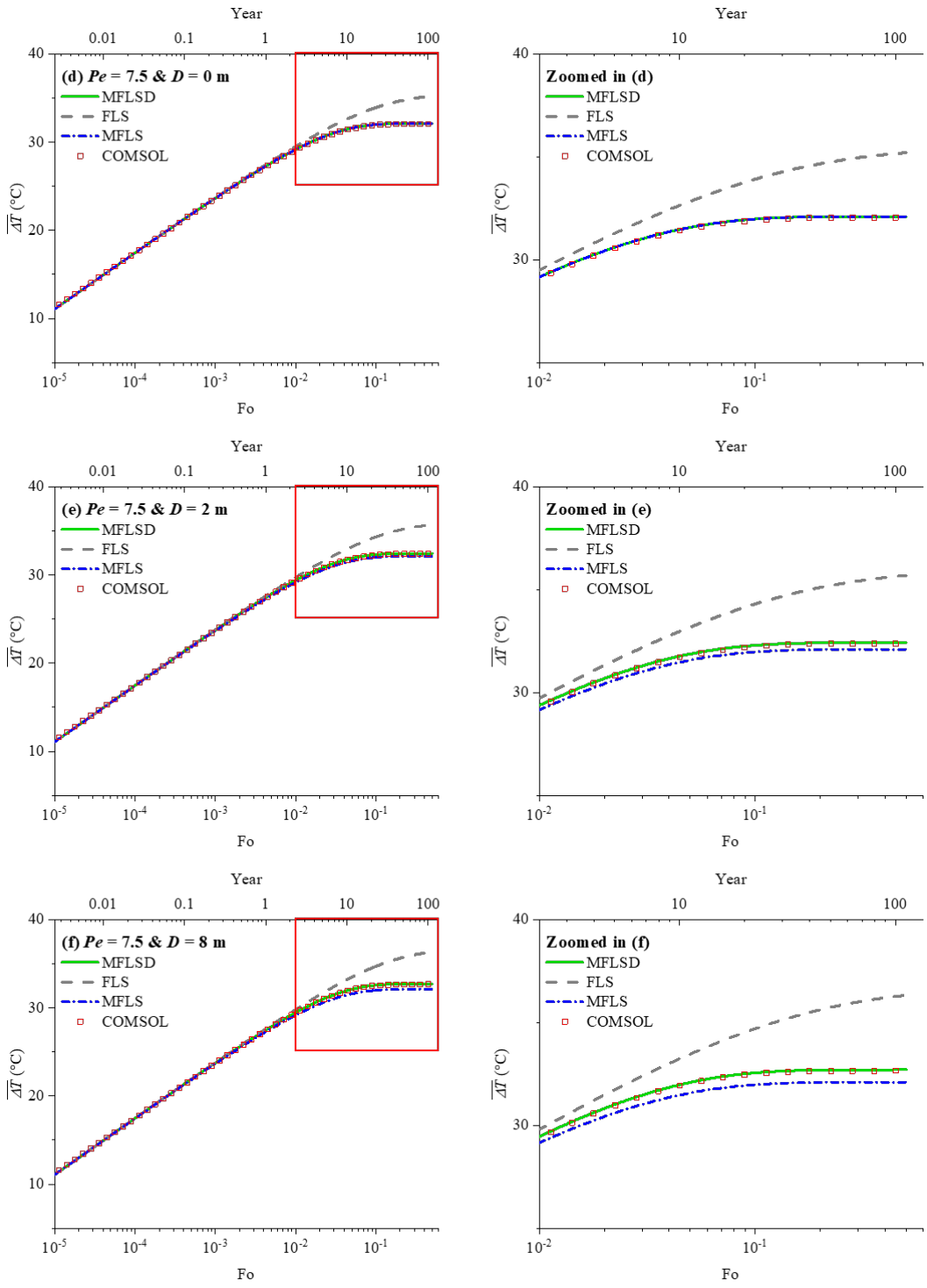

Figure 1. Borehole wall temperature variations against Fourier number for the given parameters (a) Pe = 0, D = 0 m; (b) Pe = 0, D = 2 m; (c) Pe = 0, D = 8 m; (d) Pe = 7.5, D = 0 m; (e) Pe = 7.5, D = 2 m; (f) Pe = 7.5, D = 8 m.

Table 2. MAE and MRSD between the temperature variation ($\overline{\Theta}$) predicted from analytical models and the $\overline{\Theta}$ observed from the FE COMSOL model.

		Pe = 0			*Pe* = 7.5		
		D = 0 m (**a**)	2 m (**b**)	8 m (**c**)	*D* = 0 m (**d**)	2 m (**e**)	8 m (**f**)
MAE		0.008	0.009	0.008	0.009	0.009	0.008
RMSD	FLS	0.010	0.010	0.010	0.208	0.217	0.235
	MFLS	0.010	0.010	0.010	0.010	0.010	0.010
	MFLSD	0.010	0.037	0.078	0.010	0.029	0.053

2.4.2 Computational time

Computational time is another interesting aspect used to compare analytical solutions and numerical solutions. When a program is to be executed repeatedly, its computational time determines the productivity of the given program [48]. In this paper, computational time represents the total amount of time required to execute MATLAB scripts or COMSOL simulations. In comparison, borehole wall temperature variations were computed using FLS solution [22], MFLS solution [24], MFLSD solution, and 3D-FE COMSOL solution for *D* = 2 m and *Pe* = 7.5. Other borehole geometry and thermal properties are the same as in the real case scenario.

The computational time of various time scale (i.e., hour, month, year, and decade) simulations for each analytical and numerical solution is shown in Table 3. Compared with the FLS solution, the MFLSD solution is able to account for groundwater flow without any significant drawbacks on computational time. Meanwhile, using the method given by Claesson and Javed [22], the MFLSD solution reduced the computational time of the MFLS solution by approximately 16% in monthly and hourly simulations. In comparison with COMSOL solution, the MFLSD solution reduced the computational time by a factor of ten thousand times for monthly and yearly simulation. In addition, the COMSOL model failed to finish the hourly simulation due to limited available disk space (5.4 TB). Thus, the MFLSD solution is more computationally efficient than the 3D numerical model from the viewpoint of time and space usage.

Table 1. Comparison of the computational time for the analytical and numerical solutions.

		Computational time (s)			
Time scale	Number of points	COMSOL model	FLS	MFLS	MFLSD
Hour	876000	N/A	382.62	471.80	397.01
Month	1200	6234	0.58	0.70	0.59
Year	100	3784	0.10	0.11	0.12
Decade	10	2992	0.06	0.06	0.07

2.4.3 Sensitivity study of the non-dimensional buried depth (*d*)

The new solution of the MFLS model takes the effect of buried depth into consideration. This MFLSD solution can be expressed as four variables in non-dimensional form, $R_b = r_b / H$,

$d = D/H$, Fourier number $Fo = \alpha t/H^2$, and Peclet number $Pe = UH/\alpha$. To elucidate the role of buried depth, a sensitivity study was carried out based on the identified non-dimensional variables.

2.4.3.1 Effects of non-dimensional buried depth (d) on the temperature variation at various Fo values

Fig. 2 demonstrates the non-dimensional temperature variation $\overline{\Theta_{MFLSD}}(Fo)$ obtained with the MFLSD solution for *Pe* = 0 and R_b = 0.001. According to the typical length of a vertical borehole (50 m to 150 m) and selected values of buried depth (0 m to 8 m), a ratio of $d = D/H$ varying from 0 to 0.2 was considered for these paper. Three other values (0.02, 0.05, and 0.1) were chosen within this range for a sensitivity study. In addition, a theoretical upper bound solution corresponding to $d = \infty$ was also tested [41] to set the upper limit of the solutions, although $d = \infty$ is unrealistic for practical applications. For every *d* value, $\overline{\Theta_{MFLSD}}(Fo)$ rises monotonically as *Fo* increases and eventually reaches a steady state. As shown in Table 4, as the ratio $d = D/H$ is enlarged from 0 to 0.2, the steady state value increases from 5.91 to 6.20. This increase can be explained by the thermal resistance of the ground layer above the BHE [32]. As the BHEs are buried further below the ground surface, the thermal resistance of the ground layer above the BHEs becomes larger, which reduces the heat flow between the BHEs and ground surface.

Also, it is shown in Fig. 2 that the influence of the buried depth becomes more evident for temperature variation in the long term. For example, in the beginning (*Fo = 0.001*), the value of $\overline{\Theta_{MFLSD}}$ has virtually no difference; at a steady state, the value of $\overline{\Theta_{MFLSD}}$ rises by about 5.00% when the ratio $d = D/H$ varies from 0 to 0.2 (see Table 3). According to the 1% criterion, the buried depth becomes negligible in the long term. In addition, the calculated value of $\overline{\Theta_{MFLSD}}$ is only for a single borehole in this paper. For multiple borehole configurations, the value of $\overline{\Theta_{MFLSD}}$ increases when there is a heat source interaction [41]. Therefore, it is concluded that the buried depth is a significant parameter that cannot be neglected in the generation of *g*-functions.

Table 2. Non-dimensional temperature variation for *Pe* = 0 and R_b = 0.001 with considering various *d* ranging from 0 to infinity.

	Non-dimensional temperature variation					
Fo	*d* = 0	0.02	0.05	0.1	0.2	∞
0.001	3.81	3.82	3.82	3.82	3.82	3.82
0.01	4.84	4.88	4.89	4.90	4.90	4.90
0.1	5.63	5.68	5.73	5.76	5.79	5.81
1	5.89	5.96	6.02	6.09	6.17	6.32
10	5.91	5.98	6.04	6.11	6.20	6.51

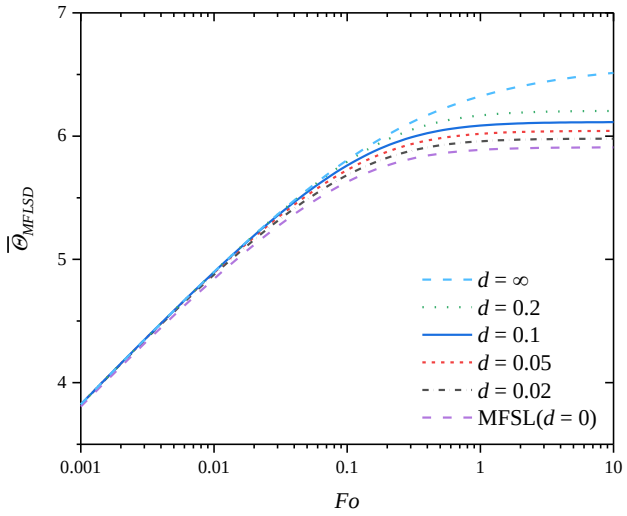

Figure 2. Non-dimensional temperature variation over time for Pe = 0 and R_b = 0.001 with considering various d values.

2.4.3.2 Effects of non-dimensional buried depth (d) on the temperature variation at various R_b values

The $\overline{\Theta_{MFLSD}}(R_b)$ was obtained with the MFLSD model for Pe = 0 with considering various d ranging from 0 to 0.2 at a steady state. Boreholes are typically 0.1 m to 0.15 m in diameter [9]. According to the typical length of a vertical borehole (50 m to 150 m), a ratio of $R_b = r_b/H$ varying from 0.0003 to 0.0015 was considered. As shown in Fig. 3a, the slopes of all the curves are similar. Therefore, the difference of two solutions ($\overline{\Theta_{MFLSD}} - \overline{\Theta_{MFLS}}$) was used to describe the discrepancy between the two solutions. Fig. 3b indicates that the difference between the two solutions is constant for any R_b values. The same phenomenon appears for any value of Fo in the considered range. In other words, the effects of buried depth are unaffected by the borehole radius.

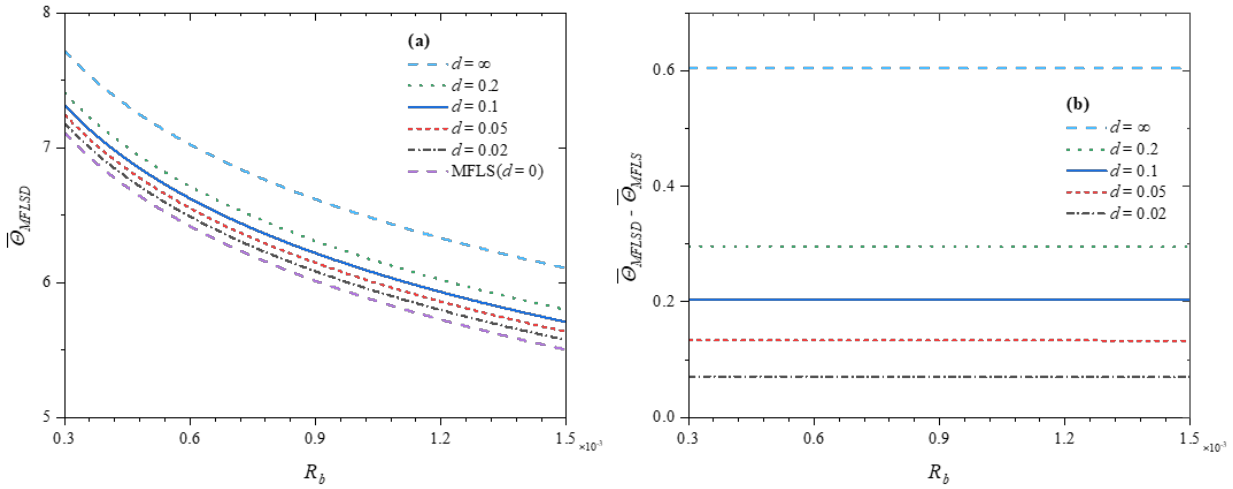

Figure 3. (a) Non-dimensional temperature variation for various d ranging from 0 to 0.2 and various R_b ranging from 0.0003 to 0.0015 at a steady state (Fo = 10) and at Pe = 0. (b) The difference between the MFLS solution and MFLSD solution for various d values.

3.4.3.3 Effects of non-dimensional buried depth (d) on temperature variation at various Pe values

To assess the influence of both groundwater flow and buried depth, another comparison between the MFLSD solution ($\overline{\Theta_{MFLSD}}$) and the MFLS solution of Tye-Gingras and Gosselin ($\overline{\Theta_{MFLS}}$) was carried out. The ratio of $\overline{\Theta_{MFLSD}}/\overline{\Theta_{MFLS}}$ was used to describe the discrepancy between the two solutions. At a steady state, the percentage difference between the two solutions for different buried depths and different Peclet numbers $0.1 < Pe < 1000$ was plotted. Fig. 4 demonstrates that the increase of the groundwater flow velocity reduces the effect of buried depth. For example, for d = 0.2, the percentage of difference between the two solutions is about 5% for Pe = 0.1, and it falls to about 0.07% for Pe = 1000. Moreover, for Pe > 100, the curves at different buried depths are in close agreement with each other, which means the effect of groundwater advection eliminates the influence of buried depth. For Pe > 22, the discrepancy between the MFLS solution and MFLSD solution for $d = \infty$ is less than 1%. Since the MFLSD solution for $d = \infty$ laid out the upper bound limit of the results [41], the percentage difference between the two solutions for any buried depth is greater than 1% for Pe < 22. Referring to the one percent criterion, the g-function must be calculated by the MFLSD solution rather than by the MFLS solution for Pe < 22.

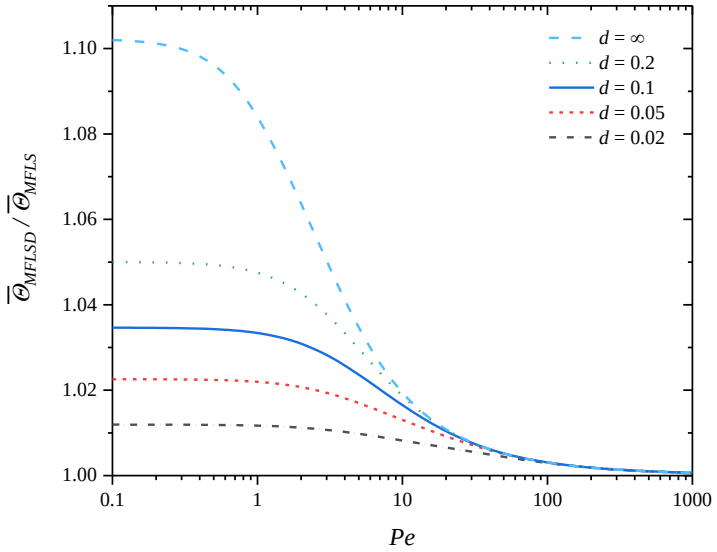

Figure 4. Percentage of difference between the MFLS solution and MFLSD solution for various buried depths and various Peclet numbers.

2.4.4 Influence of buried depth at fixed borehole lengths

Although the aforementioned non-dimensional variables have obvious advantages, parameters with physical meanings, including buried depth, borehole length, and operation time, are of great concern in engineering design. The MFLSD solution was simulated for common borehole lengths ranging from 50 m to 150 m and for Pe = 0. For each fixed borehole length, the buried depth varied from 0 m to 8 m. Other borehole geometries and thermal properties were the same as in the real geoexchange system project. The simulation was run for 30 years, which is the expected lifetime of GSHP systems [49]. The temperature variations were calculated using Eq. (10), and then the values were recast in non-dimensional forms.

By analyzing the $\overline{\Theta_{MFLSD}}$ against the time in years for Pe = 0 (as shown in Fig. 5), it can be demonstrated that the impact of buried depth gets larger as the borehole length reduces. For example, compared with the standard MFLS model (D = 0 m), the $\overline{\Theta_{MFLSD}}$ rises by 1.12% for a 150 m borehole that starts from 8 m below the surface, and it rises by 3.55% if the borehole is only 50 m in length. The other Peclet number scenario (Pe = 7.5) was also calculated. Although the influence of groundwater flow reduces the effects of buried depth, $\overline{\Theta_{MFLSD}}$ still rises by 2.62% for a 50 m borehole at D = 8 m. Thus, referring to the one percent criterion, the buried depth becomes an important parameter for the design of short BHEs. This conclusion is not fully consistent with Eskilson's original work [11]. Eskilson concluded that the exact value of buried depth is not important since only small temperature variations (i.e., 0.1 °C) were found for a buried depth of 2 m to 8 m with a fixed active borehole length. Eskilson's conclusion is adequate for longer boreholes, but it is inadequate for a shallow borehole. As shown in Table 5, for a 150 m borehole, temperature variation increases by 0.58% when the buried depth varies from 2 m to 8 m. for a 50 m borehole, the percentage difference is 1.83% between the temperature variations with D = 2 m and D = 8 m. When the percentage difference is greater than 1%, the exact value of buried depth must be taken into account. To summarize, in practical application, buried depth is

a significant parameter in the design of short BHEs. The exact value of buried depth cannot be neglected.

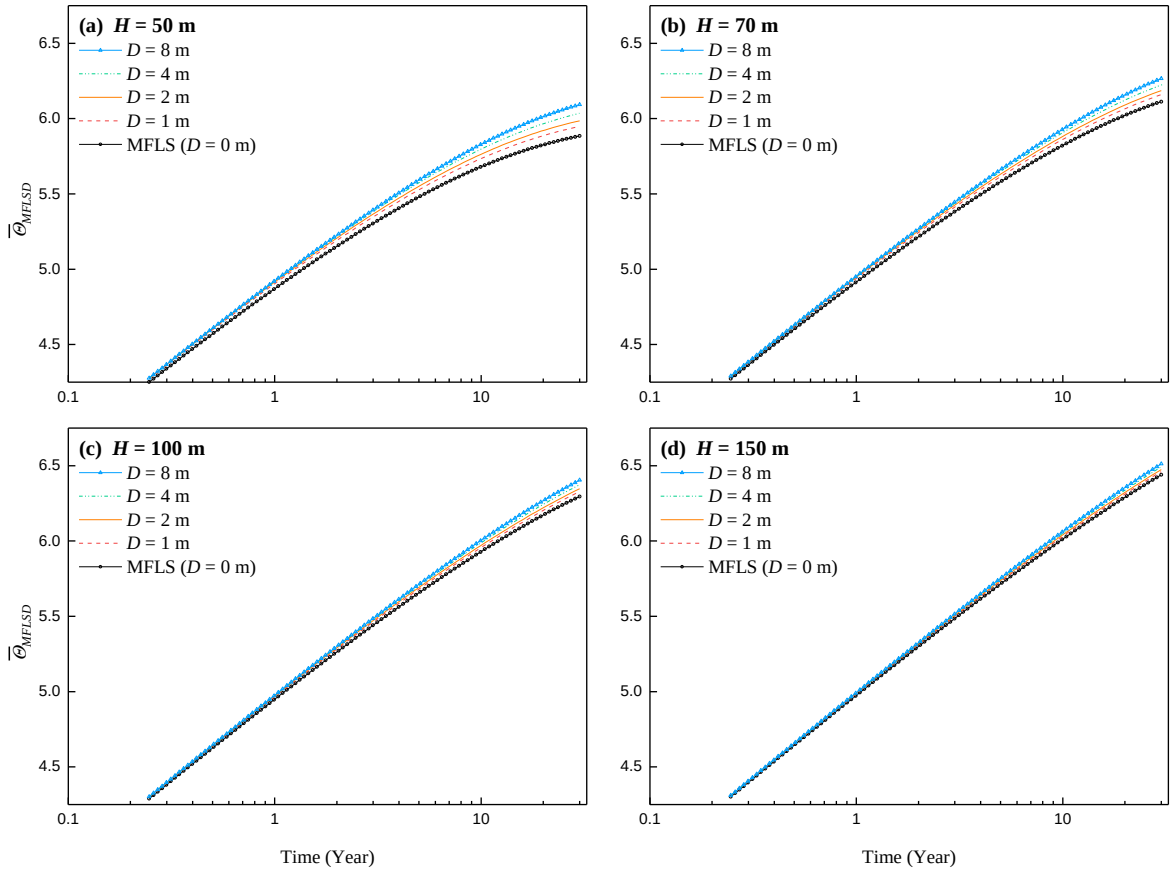

Figure 5. Temperature variations over time for Pe = 0 (a) H = 50 m, (b) H = 70 m, (c) H = 100 m, (d) H = 150 m.

Table 3. Non-dimensional temperature variation for different buried depths and groundwater flow scenarios at 30 years.

	Non-dimensional temperature variations				% Difference ($\overline{\Theta_{MFLSD}}/\overline{\Theta_{MFLS}}-1$)			
Pe = 0	*H* = 50 m	70 m	100 m	150 m	50 m	70 m	100 m	150 m
MFLS (*D* = 0 m)	**5.88**	**6.11**	**6.30**	**6.44**	**Ref**			
D = 1 m	5.95	6.16	6.33	6.46	1.08%	0.76%	0.52%	0.34%
2 m	5.99	6.19	6.35	6.47	1.72%	1.21%	0.83%	0.54%
4 m	6.04	6.22	6.37	6.49	2.57%	1.82%	1.24%	0.81%
8 m	6.09	6.27	6.40	6.51	3.55%	2.51%	1.72%	1.12%
Pe = 7.5	*H* = 50 m	70 m	100 m	150 m	50 m	70 m	100 m	150 m
MFLS (*D* = 0 m)	**5.57**	**5.72**	**5.83**	**5.92**	**Ref**			
D = 1 m	5.62	5.75	5.86	5.94	0.95%	0.66%	0.46%	0.30%
2 m	5.65	5.77	5.87	5.94	1.44%	1.01%	0.70%	0.46%
4 m	5.68	5.80	5.89	5.96	2.04%	1.43%	0.99%	0.65%
8 m	5.72	5.82	5.90	5.97	2.62%	1.84%	1.27%	0.83%

2.5 Project outcomes

From the project, a refined analytical solution has been developed to consider both the groundwater and buried depth.

2.6 Important lessons learned

(1) The development of the MFLSD solution is based on the homogeneous ground assumption: the ground is assumed to be uniform along the vertical depth of a borehole. In practical applications, the boreholes are normally drilled through different layers, and these layers have different thermal properties and the hydro-geological conditions. Particularly, water table (the upper surface of the zone of the saturated ground) is generally found at a certain depth underneath the ground surface, and the water table fluctuates seasonally and from year to year. Therefore, the homogeneous assumption can lead to unreliable results. To avoid the associated limitation of homogeneous ground assumption, multiple ground layers will be taken account into the MFLSD solution in the future study.

(2) The development of line source model assumes that a constant heat flux is applied along the borehole length, i.e. constant heat flux boundary condition, and the temperature on the borehole wall changes accordingly. On the other hand, another boundary condition, uniform temperature boundary condition, is also commonly used for generating *g*-functions [36, 37, 50]. The uniform temperature boundary condition assumes that a uniform temperature is applied along the borehole length and all boreholes have the same temperature at the borehole wall [36]. Note that Eskilson's *g*-functions were computed using the uniform temperature boundary condition [11]. An dispersion between the Eskilson's *g*-functions and the analytical *g*-functions, which obtained from the FLS model with the constant heat flux boundary condition, was observed [25, 36, 50, 51]. The dispersion is greater for larger borehole fields [36]. For example, Monzo et al. [50] found that the difference between the

results with the two different boundary conditions are virtually insignificant for a small multiple borehole field of 2 × 3 boreholes, and Cimmino and Bernier [36] found that the differences become 52% at the steady state for a large multiple borehole field of 10 × 10 boreholes. However, no work has been done to determine which boundary condition has a better agreement with the practical condition. Therefore, future study will be devoted to evaluating the differences between the practical condition and the two assumed boundary conditions.

3. Greenhouse Gas and Non-GHG Impacts

3.1 Qualitative discussion about the GHG benefits

GeoExchange system needs 30–50% less energy consumption (~ 0.22 - 0.35 kWh electricity per kWh cooling/heating load), when compared with the conventional air-sourced heat pumps, leading to an indirect 30–50% reduction of GHG emissions, correspondingly.

3.2 Quantification of expected annual GHG benefits projected

The indirect reduction of GHG emissions has been quantified by some researchers. For example, Hanova et al. (2007) compared the GHG emissions (CO_2 eq) of GeoExchange system with conventional heating systems across Canada; the results show that Alberta has the most significant potential to reduce GHG emissions—22.3 tons per year for an average Canadian home (area ~140 m^2)—from the GeoExchange system.

The results from this project will reduce the capital costs of the GeoExchange system and increase its number of installations—this will occur through a knowledge dissemination plan—through journal and conference papers. According to Statistics Canada (2011), there are 1,390,275 households in Alberta. It is estimated that, with a 10% of the households having the GeoExchange system, the reduction of GHG emissions will be about 3 Mt per year in Alberta, which is 1% of the total GHG emission (~275 Mt) of Alberta in 2015.

Reference: Hanova, J., Dowlatabadi, H. & Mueller, L. 2007. Ground Source Heat Pump Systems in Canada: Economics and GHG Reduction Potential. *Resources for the Future***,** 1-37.

3.3 Discussion about the immediate and potential future non-GHG benefits

Since the GeoExchange system is increasingly popular across Canada, the outcome of this research can be directly used in other nationwide projects. The findings of this research could be used to improve the design of BHE and the GeoExchange system, leading to more economically feasible design. Moreover, the influence of groundwater flow from analytical and numerical models has be quantitatively compared and examined. As a result, a refined approach has been proposed to guide future design projects that will have better performance. In addition, a more efficient GeoExchange System will be developed to reduce emissions.

4. Overall Conclusions

The following conclusions were drawn from the study:

1) A new single integral solution of the moving finite line source (MFLS) model was generated to consider the effect of buried depth. The new solution (MFLSD) gives the average temperature variation over the borehole surface at any borehole radius. The MFLSD solution is numerically verified with a three-dimensional (3D) finite-element (FE) COMSOL model. Compared with the 3D-FE COMSOL model, the MFLSD solution is more computationally efficient from the viewpoint of time and space usage.
2) In general, both groundwater flow and buried depth have certain effects on the temperature variation of a borehole heat exchanger (BHE) in a long-time simulation. The effect of buried depth diminishes heat transfer between the ground surface and BHE, and the effect of groundwater flow balances the accumulated heat in the ground gradually. The MFLSD solution, incorporating the effects of buried depth and groundwater flow at the same time, provides a more accurate estimation of the *g*-function, leading to a more thermal-effective design.
3) The effect of buried depth heavily depends on the groundwater velocity. The increase of the groundwater flow velocity reduces the effect of buried depth. In a very high groundwater flow velocity scenario (i.e., $Pe > 100$), the effect of groundwater advection eliminates the influence of buried depth. For $Pe < 22$, the MFLSD solution must be used over the standard MFLS model to consider the combined effects of buried depth and groundwater flow when calculating temperature variation.
4) The impact of buried depth increases with regard to long-term temperature variation as the borehole length reduces. For the given parameters in this paper, for a long borehole (H = 150 m), the average non-dimensional temperature rises by about 1.12% as buried depth increases from 0 m to 8 m; for a short borehole (H = 50 m), the non-dimensional temperature rises by about 3.55% with the same change in buried depth. In practical applications, buried depth is a significant parameter in the design of short BHEs; the exact value of buried depth cannot be neglected.
5) The effects of buried depth would be more significant in a borehole field containing multiple boreholes due to the accumulation effects of the buried boreholes. This MFLSD solution will be combined with a spatial superposition procedure to compute the *g*-functions of the borehole field in further studies.

5. Scientific Achievements

This project has delivered 2 presentations (C1 and C2), 1 conference paper (C2), 1 journal paper (J1), and 1 MSc thesis (T1). The asterisks (*) indicates the HQP under this project.

J1) Guo Y*, Hu X*, Banks J, **Liu W**. (2019). Considering buried depth in the moving finite line source model for vertical borehole heat exchangers—a new solution. *Energy and Buildings,* © Elsevier (under review) (IF = 4.823)

C1) Guo Y***** (presenter), Komar K, **Liu W**, Sepehri M*. (2018). Considering groundwater advection on the design of borehole heat exchanger—a review of analytical solutions. GeoEdmonton, Edmonton, Canada. pp. 1-7

C2) Guo Y* (presenter), **Liu W**. (2018). Considering groundwater advection on the design of borehole heat exchanger—a review of analytical solutions. Faculty of

Engineering Graduate Student Symposium - University of Alberta. Edmonton, Canada.

T1) Guo Y*. (2019). Considering buried depth in the moving finite line source model for vertical borehole heat exchangers—a new solution. *MSc Thesis, University of Alberta.* 106 pages

For the first time, a new single integral solution of the moving finite line source (MFLS) model was generated to consider the effect of both ground water and buried depth. The new solution (MFLSD) gives the average temperature variation over the borehole surface at any borehole radius. The MFLSD solution is verified numerically with a three-dimensional (3D) finite-element (FE) COMSOL model. Compared with the 3D-FE COMSOL model, the MFLSD solution is more computationally efficient from the viewpoint of time and space usage.

7. Next Steps

7.1 Next steps for the technology/process/innovation

Continuing research is in progress with the collaboration from the Future Energy Systems - Canada First Research Excellence Fund (CFREF). The MSc student graduated in Sept 2019, and he is now a PhD student continuing the research to refine the design approach of GeoExchange system.

7.2 Long-term plan for commercialization

The design approach of BHE will be further improved to consider multiple layers of lithology and non-uniform heat flux boundaries conditions. 3 years later, a new design framework will be published and then the framework can be used by BHE designers across Alberta, Canada, and the world.

7.3 Potential partnerships

Potential partnerships may be established with the Parkland County, which has shown strong interest to utilize the GeoExchange system—the shallow geothermal energy.

8. Communications plan

The best way to communicate the results is through scientific publications and conferences. Continuous efforts will be made to dissimilate the research results from this project.

References

[1] H. Yang, P. Cui, Z. Fang, Vertical-borehole ground-coupled heat pumps: A review of models and systems, Applied Energy, 87 (1) (2010) 16-27.
[2] J. Luo, J. Rohn, M. Bayer, A. Priess, Thermal efficiency comparison of borehole heat exchangers with different drillhole diameters, Energies, 6 (8) (2013) 4187-4206.
[3] H. Carslaw, J. Jaeger, Heat in solids, Clarendon Press, Oxford, 1959.
[4] T.V. Bandos, Á. Montero, E. Fernández, J.L.G. Santander, J.M. Isidro, J. Pérez, P.J.F.d. Córdoba, J.F. Urchueguía, Finite line-source model for borehole heat exchangers: effect of vertical temperature variations, Geothermics, 38 (2) (2009) 263-270.
[5] N.R. Diao, Q.Y. Li, Z.H. Fang, Heat transfer in ground heat exchangers with groundwater advection, Int J Therm Sci, 43 (12) (2004) 1203-1211.
[6] I. Sarbu, C. Sebarchievici, General review of ground-source heat pump systems for heating and cooling of buildings, Energy and Buildings, 70 (2014) 441-454.
[7] U. Lucia, M. Simonetti, G. Chiesa, G. Grisolia, Ground-source pump system for heating and cooling: Review and thermodynamic approach, Renewable and Sustainable Energy Reviews, 70 (2017) 867-874.
[8] M.A. Bernier, Closed-loop ground-coupled heat pump systems, Ashrae Journal, 48 (9) (2006) 12.
[9] ASHRAE, 34 Geothermal energy, in: 2015 ASHRAE Handbook - Heating, Ventilating, and Air-Conditioning Applications (SI Edition), American Society of Heating, Refrigerating and Air-Conditioning Engineers, Inc., 2015.
[10] S. Miglani, K. Orehounig, J. Carmeliet, A methodology to calculate long-term shallow geothermal energy potential for an urban neighbourhood, Energy and Buildings, 159 (2018) 462-473.
[11] P. Eskilson, Thermal analysis of heat extraction boreholes, (1987).
[12] M. Li, A.C.K. Lai, Review of analytical models for heat transfer by vertical ground heat exchangers (GHEs): A perspective of time and space scales, Applied Energy, 151 (Supplement C) (2015) 178-191.
[13] A. Priarone, M. Fossa, Modelling the ground volume for numerically generating single borehole heat exchanger response factors according to the cylindrical source approach, Geothermics, 58 (2015) 32-38.
[14] J.D. Spitler, GLHEPRO-A design tool for commercial building ground loop heat exchangers, in: Proceedings of the fourth international heat pumps in cold climates conference, Citeseer, 2000.
[15] G. Hellström, B. Sanner, Earth energy designer, User's Manual, version, 2 (2000).
[16] D. Bauer, W. Heidemann, H.J.G. Diersch, Transient 3D analysis of borehole heat exchanger modeling, Geothermics, 40 (4) (2011) 250-260.
[17] P. Monzó, A.R. Puttige, J. Acuña, P. Mogensen, A. Cazorla, J. Rodriguez, C. Montagud, F. Cerdeira, Numerical modeling of ground thermal response with borehole heat exchangers connected in parallel, Energy and Buildings, 172 (2018) 371-384.
[18] C. Yavuzturk, J.D. Spitler, S.J. Rees, A transient two-dimensional finite volume model for the simulation of vertical U-tube ground heat exchangers, ASHRAE transactions, 105 (2) (1999) 465-474.
[19] P. Monzó, Comparison of different Line Source Model approaches for analysis of Thermal Response Test in a U-pipe Borehole heat Exchanger, in, 2011.

[20] H.Y. Zeng, N.R. Diao, Z.H. Fang, A finite line‐source model for boreholes in geothermal heat exchangers, Heat Transfer—Asian Research, 31 (7) (2002) 558-567.
[21] L. Lamarche, B. Beauchamp, A new contribution to the finite line-source model for geothermal boreholes, Energy and Buildings, 39 (2) (2007) 188-198.
[22] J. Claesson, S. Javed, An analytical method to calculate borehole fluid temperatures for time-scales from minutes to decades, in: ASHRAE Transactions, 2011, pp. 279-288.
[23] N. Molina-Giraldo, P. Blum, K. Zhu, P. Bayer, Z. Fang, A moving finite line source model to simulate borehole heat exchangers with groundwater advection, Int J Therm Sci, 50 (12) (2011) 2506-2513.
[24] M. Tye-Gingras, L. Gosselin, Generic ground response functions for ground exchangers in the presence of groundwater flow, Renewable Energy, 72 (2014) 354-366.
[25] M. Cimmino, B.R. Baliga, A hybrid numerical-semi-analytical method for computer simulations of groundwater flow and heat transfer in geothermal borehole fields, Int J Therm Sci, 142 (2019) 366-378.
[26] M. Samson, J. Dallaire, L. Gosselin, Influence of groundwater flow on cost minimization of ground coupled heat pump systems, Geothermics, 73 (2018) 100-110.
[27] A. Capozza, M. De Carli, A. Zarrella, Investigations on the influence of aquifers on the ground temperature in ground-source heat pump operation, Applied Energy, 107 (2013) 350-363.
[28] J. Hecht-Méndez, M. de Paly, M. Beck, P. Bayer, Optimization of energy extraction for vertical closed-loop geothermal systems considering groundwater flow, Energy Conversion and Management, 66 (2013) 1-10.
[29] M. de Paly, J. Hecht-Méndez, M. Beck, P. Blum, A. Zell, P. Bayer, Optimization of energy extraction for closed shallow geothermal systems using linear programming, Geothermics, 43 (2012) 57-65.
[30] J. Hu, An improved analytical model for vertical borehole ground heat exchanger with multiple-layer substrates and groundwater flow, Applied Energy, 202 (2017) 537-549.
[31] M. Fossa, A fast method for evaluating the performance of complex arrangements of borehole heat exchangers, HVAC&R Research, 17 (6) (2011) 948-958.
[32] M. Cimmino, M. Bernier, F. Adams, A contribution towards the determination of g-functions using the finite line source, Applied Thermal Engineering, 51 (1-2) (2013) 401-412.
[33] L. Ingersioll, O.J. Zobel, A.C. Ingersoll, Heat Conduction: With Engineering Geological And Other Applications, Oxford And Ibh Publishing Co.; Calcutta; Bombay; New Delhi, 1954.
[34] J.A. Rivera, P. Blum, P. Bayer, A finite line source model with Cauchy-type top boundary conditions for simulating near surface effects on borehole heat exchangers, Energy, 98 (2016) 50-63.
[35] S. Erol, B. François, Multilayer analytical model for vertical ground heat exchanger with groundwater flow, Geothermics, 71 (Supplement C) (2018) 294-305.
[36] M. Cimmino, M. Bernier, A semi-analytical method to generate g-functions for geothermal bore fields, International Journal of Heat and Mass Transfer, 70 (2014) 641-650.
[37] L. Lamarche, g-function generation using a piecewise-linear profile applied to ground heat exchangers, International Journal of Heat and Mass Transfer, 115 (2017) 354-360.
[38] J.D. Spitler, M. Bernier, 2 - Vertical borehole ground heat exchanger design methods, in: S.J. Rees (Ed.) Advances in Ground-Source Heat Pump Systems, Woodhead Publishing, 2016, pp. 29-61.
[39] P. Eslami-nejad, M. Bernier, Freezing of geothermal borehole surroundings: A numerical and experimental assessment with applications, Applied Energy, 98 (2012) 333-345.

[40] G. Dalla Santa, Z. Farina, H. Anbergen, W. Rühaak, A. Galgaro, Relevance of computing freeze-thaw effects for borehole heat exchanger modelling: A comparative case study, Geothermics, 79 (2019) 164-175.
[41] T.V. Bandos, Á. Campos-Celador, L.M. López-González, J.M. Sala-Lizarraga, Finite cylinder-source model for energy pile heat exchangers: Effect of buried depth and heat load cyclic variations, Applied Thermal Engineering, 96 (2016) 130-136.
[42] S. Gehlin, Thermal response test: method development and evaluation, Luleå tekniska universitet, 2002.
[43] A.D. Chiasson, S.J. Rees, J.D. Spitler, A preliminary assessment of the effects of groundwater flow on closed-loop ground source heat pump systems, in, Oklahoma State Univ., Stillwater, OK (US), 2000.
[44] H. Fujii, R. Itoi, J. Fujii, Y. Uchida, Optimizing the design of large-scale ground-coupled heat pump systems using groundwater and heat transport modeling, Geothermics, 34 (3) (2005) 347-364.
[45] H. Wang, C. Qi, H. Du, J. Gu, Thermal performance of borehole heat exchanger under groundwater flow: A case study from Baoding, Energy and Buildings, 41 (12) (2009) 1368-1373.
[46] M.G. Sutton, D.W. Nutter, R.J. Couvillion, A ground resistance for vertical bore heat exchangers with groundwater flow, Journal of Energy Resources Technology, 125 (3) (2003) 183-189.
[47] E. Zanchini, S. Lazzari, A. Priarone, Long-term performance of large borehole heat exchanger fields with unbalanced seasonal loads and groundwater flow, Energy, 38 (1) (2012) 66-77.
[48] A.V. Aho, J.D. Ullman, Foundations of computer science, Computer Science Press, 1995.
[49] B. Huang, V. Mauerhofer, Life cycle sustainability assessment of ground source heat pump in Shanghai, China, Journal of Cleaner Production, 119 (2016) 207-214.
[50] P. Monzó, P. Mogensen, J. Acuña, F. Ruiz-Calvo, C. Montagud, A novel numerical approach for imposing a temperature boundary condition at the borehole wall in borehole fields, Geothermics, 56 (2015) 35-44.
[51] M. Fossa, The temperature penalty approach to the design of borehole heat exchangers for heat pump applications, Energy and Buildings, 43 (6) (2011) 1473-1479.